CUMM D65 0130

active K^{40}. Although the same radionuclides were reported in core samples from this general area (6), the *in situ* spectra are clearly superior. The large "sample size" assures an increased counting rate that more than compensates for the loss of detail resulting from the effects of the water on the γ-ray photons.

Comparison of a spectrum of coarse sand and gravel, in 30 m of water 1.6 km off Newport, Oregon (Fig. 2*b*), shows no radionuclides resulting from operations at the Hanford laboratories. The plume of the Columbia River does not normally move into this area, although marine animals taken here contain Zn^{65} (7). Most deposits of silts and clays in the northeast Pacific Ocean, which might have larger amounts of artificial radioactivity than sands and gravels, are beyond the present range of our probe. Range is restricted by the 54-m cable used in these tests, but Riel (8) has shown that longer cable lengths are feasible. The probe housing was designed for and tested at much greater pressures, and the only modifications required are in the cable length and associated electronics. These modifications are in progress and should let us work down to about 400 m.

Our interest lies in the relationship of the radioactivity of animals to that of their environment. Analysis techniques for animals are relatively simple, since the specific activity of the samples can be increased by ashing, with the ash counted in the well of a NaI(Tl) crystal (12.5 by 12.5 cm) in the laboratory. There is no easy comparable method of concentrating the radioactivity in sediment samples. The difficulties inherent in the collection and subsequent radioanalysis of sediments seem to make methods of probing *in situ* worthy of further effort.

DAVID JENNINGS
NORMAN CUTSHALL
CHARLES OSTERBERG
Department of Oceanography, Oregon State University, Corvallis

References and Notes

1. The actual depth to which the probe "sees" depends on both the energy of the γ-ray emitters and the density of the matrix material. Therefore, the effective size of the sample would be less for Cr^{51} (0.32 Mev) than for K^{40} (1.46 Mev).
2. J. H. Harley, Ed., *Operation* Troll: *Joint preliminary report* (HASL, U.S. Atom. Energy Comm., New York Operations Office, NYO 4656, April 1956).
3. C. M. Proctor, E. Papadopulos, R. H. Firminhac, *Limnol. Oceanogr.* **7**, 280 (1962).
4. M. G. Gross, C. A. Barnes, G. K. Riel, in preparation.
5. P. C. Klingeman and W. J. Kaufman, "Transport of radionuclides with San Francisco Bay sediments," Progress Report 1961-1962 Water Year. *Sanitary Eng. Res. Lab. Rep.* No. 63-7, (Univ. of California, Berkeley, 1963), p. 70.
6. C. Osterberg, J. Byrne, V. Kulm, *Science* **139**, 916 (1963).
7. C. Osterberg, J. Pattullo, W. Pearcy, *Limnol. Oceanogr.* **9**, 249 (1964).
8. G. K. Riel, *Electronics* **36**, No. 10, 56 (8 Mar. 1963).
9. Support from U.S. AEC contract AT(45-1)1750 and PHS training grant 1T1-WP-59-01. The data are a result of thesis research for a master's degree from Oregon State University. We thank R. S. Mesecar and W. E. Bales for design of the electronic circuitry and suggestions for waterproofing the probe.

23 February 1965

Kink-Bands: Shock Deformation of Biotite Resulting from a Nuclear Explosion

D. Cummings

Abstract. *Microscopic examination of granodiorite samples from the shock region around a nuclear explosion reveals sharply folded lens-shaped zones (kink-bands) in the mineral biotite. Fifty percent of these zones are oriented approximately 90° to the direction of shock-wave propagation, but other zones are symmetrically concentrated at shear angles of 50° and 70° to the direction of shock-wave propagation.*

In 1962, a 5.2-kiloton nuclear device was detonated in the granodiorite of the Climax stock, Nevada Test Site (Hardhat event). Deformation of biotite in the form of sharply folded lens-shaped zones (kink-bands) was observed by microscopic examination of samples affected by the shot. As a basis for defining explosion-produced effects, samples taken prior to the detonation were examined and compared with those taken after the shot (postshot samples). The locations in the reentry tunnel where the postshot samplings were made and the drill core are shown in Fig. 1.

All thin sections cut from the six samples in the reentry tunnel were oriented by having the planar dimension of the section parallel to a radius drawn from the shot point. Although the orientation for most sections cut from the postshot drill core was not known (because of rotation of the sample in the core barrel during drilling), sections from the four samples C_8, C_9, C_{10}, and C_{11} could be oriented parallel to a radius from the shot point.

Of the ten oriented postshot sections only the eight within the shock zone (*1*) displayed kink-bands (Fig. 1). These eight were examined for preferred directions of kink-bands. Of the 110 observed kink-bands in the ori[...] sections, 50 percent were oriented [...] the long axis of the lens at 90° [...] to a radius drawn from the shot [...] (Fig. 2*A*). Approximately 12 pe[...] and 10 percent were oriented wit[...] long axis of lens at 50° ± 1° [...] 70° ± 1°, respectively, from the r[...] (Fig. 2*B*).

Because only the eight oriented [...]ples within the shock zone showed [...] bands, the explosion-produced [...] wave was probably the (compre[...] stress which formed the kink-bands [...] shock wave passes spherically out[...] from the shot point so that its [...] moves along radii drawn from the [...] point. The kink-band orientation [...] thus be related to the direction of [...] propagation. The unoriented se[...] can be oriented by assuming tha[...] greatest percentage of kink-ban[...] normal to the direction of shock [...] propagation.

A total of 701 kink-bands [...] oriented and unoriented sections [...] counted. Their frequencies and o[...]tions with respect to the shock [...] are shown on Fig. 3. The relativ[...]quencies of the principal orien[...] for the unoriented sections ar[...] same as those from the oriente[...]tions. This suggests that the r[...] for deducing the direction of [...] wave propagation in unoriented [...]tions is not greatly in error.

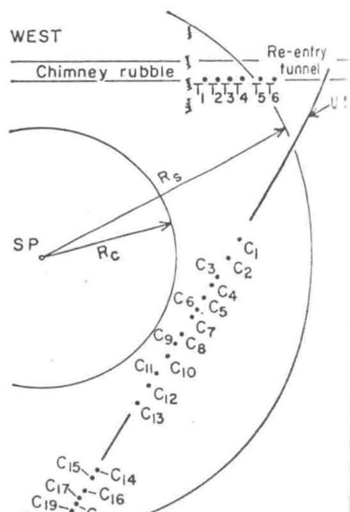

Fig. 1. Cross-sectional diagra[m] [...] vicinity of the Hardhat event [...] the reentry tunnel, postshot [...] (U15G), shock-zone radius (R_s), [...] radius (R_c), shot point (SP), [...] locations in the tunnel (T_1 [...] drill hole ($C_1 \cdots C_{22}$).

3 shows the greatest concen- kink-bands with their long al to the direction of shock- gation. The second greatest ions of kink-bands are sym- disposed at angles of 50° to the shock-wave direction. ientation of kink-bands to ve stress is illuminated by ex- al work. Griggs, Turner, and) showed that the long axis ands in biotite in an experi- deformed granite tended to normal to the axis of compres- erson and Weiss (*3*), in experi- udies of phyllite, found con- ts of kink-bands symmetrically at 50° to the direction of in specimens compressed the foliation, but only one oped in specimens compressed nd 45° to the foliation. These y studies suggest that orienta- h normal and at a moderate the axis of compression are as primary deformation fea- Ramsey (*4*) suggested that a rder shear, resulting from a ment of the principal stress s, accounts for the develop- shear folds (similar to kink-

e experiments (*2*, *3*) might read- in the concentrations at 90° Neither experiment, however, the 70° concentrations. As d by Ramsey (*4*), it may be to explain the 70° concentra- second-order shear.

stry (*5*) and Moody and Hill bed the expected geometry of ion resulting from a compres- ss. If the direction of the com- stress (shock wave) is given with y shear angle at 50°, and if cal angle" (*6*) is set to 20°, entration at 70° may be ex- as resulting from second-order g. 4).

ted above, it is believed that ck wave (and, therefore, the med the kink-bands. Although e of the shock wave is super- , and the development of der shears requires some time distribution of internal stresses, eless seems possible to argue e kink-bands resulted from a mary stress—the shock wave. 5 qualitatively shows the pas- e shock wave from the deto- oint, *0*, to the edge of the e (R_s). The history of kink- mation at a point may be

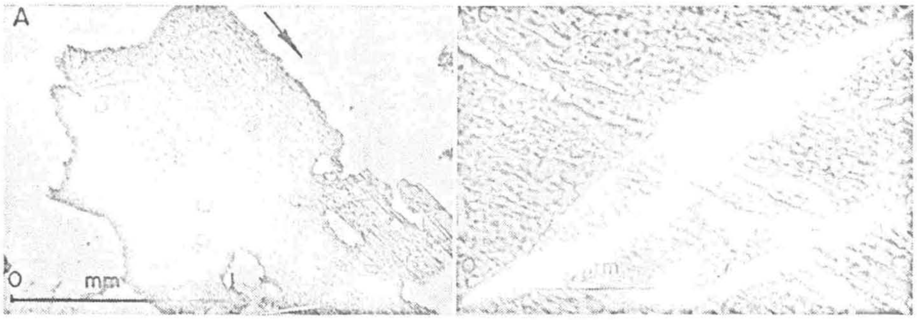

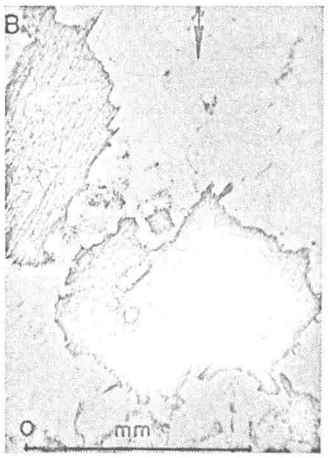

Fig. 2. Photomicrographs (plane polarized light) showing kink-bands in biotite. Arrows indicate stress direction (shock-wave propagation). Thin sections from core samples C_{10} and C_{11} used for photographs have known orientations with respect to the shot point. *A*, Kink-bands developed normal to stress direction. Crystallographic orientation of biotite with respect to the plane of the thin section is almost parallel to (001). The small black lines in the biotite almost parallel to direction of stress are inclusions. *B*, Kink-bands developed normal to stress direction (upper left and left center), at 50° (left center), and 70° (center). Other kink-bands are developed between 10° and 30° (center). Crystallographic orientation with respect to the plane of the thin section of both biotite grains is almost perpendicular to (001). Examination of thin sections prior to shot revealed no kink-bands and no apparent preferred orientation of biotite grains. *C*, Higher magnification photomicrograph of upper portion of *A* showing details of kink-bands.

related to the passage of the shock wave in time, distance, and peak compressive stress. The shock-wave front passes point *A* at time T_1, forming kink-bands normal to the direction of shock-wave propagation (90°) and primary shear sets (50°). The pressure behind the wave front does not return to ambient immediately after the passage of the front. For point *B* and time T_2, a similar argument can be proposed. At point *A* and time T_2, however, there is overpressure remaining which may be sufficient both in time

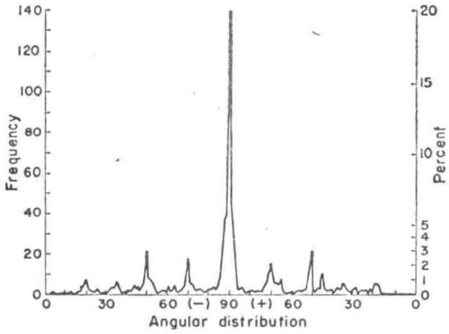

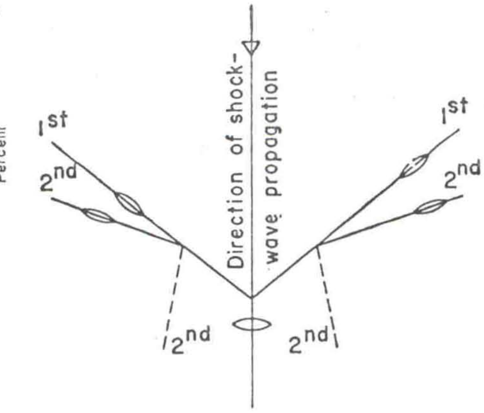

Fig. 3 (left). Frequency distribution of kink-band orientations with respect to dominant orientation. The dominant kink-band orientation, based on 110 measurements from oriented sections, is at 90° to the direction of shock-wave propagation. Kink-bands making angles in a counterclockwise direction with respect to the dominant orientation are plotted as (+); those making angles in a clockwise direction with respect to the dominant orientation are plotted as (−). Fig. 4 (right). Theoretical directions of first- and second-order shears with respect to the direction of stress (shock-wave propagation) (*6*). Dominant set of kink-bands is formed normal to the direction of shock-wave propagation. Observed concentrations of kink-band orientations interpreted as shear are indicated by solid lines. Although four directions of second-order shearing are possible, only two are present. Dashed lines indicate undeveloped shear directions. Kink-band orientations with respect to direction of shock-wave propagation and shear directions are indicated by shape of lens.

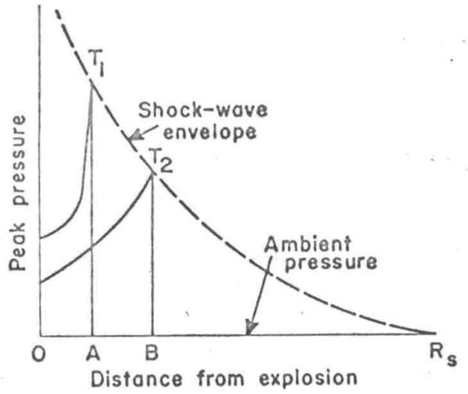

Fig. 5. Diagram of shock-wave propagation (*8*).

and magnitude to reorient the local stress field, thereby creating the second-order shears required to develop the 70° concentrations.

There does not seem to be a relation between the formation of kink-bands and the relation of the direction of the crystallographic axes of the biotite to the direction of shock-wave propagation. Whereas previous workers (*2*) suggested that kink-bands tended to develop preferentially in grains whose [001] axes [that is, normals to (001)] are steeply inclined to the compression axis, the present work indicates no such preference. Rather, in the shock zone of a nuclear explosion, kink-bands in biotite can be formed almost without regard to the crystallographic orientation. One difference in the conditions of the laboratory experiment (*2*) and the nuclear explosion which may account for the indiscriminate development of kink-bands with respect to the crystallographic axes is that the stress produced by the nuclear explosion's shock wave is of such a large magnitude and rapid application that the crystallographic anisotropy of biotite has little influence on kink-band formation.

The mode of failure, under the extremely rapid dynamic loading of a shock wave from a nuclear explosion, may be quite different from the mode of failure under the essentially static loading applied in laboratory experiments. The mode of failure, therefore, may not follow the same preferred crystallographic orientation under shock loading as under static loading.

DAVID CUMMINGS*

U.S. Geological Survey,
Denver, Colorado

References and Notes

1. The radius of the shock zone for the granodiorite, R_s, may be obtained by using the scaling formula $R_s = 75\ W^{1/3}$, where W is the yield of the nuclear explosive in terms of trinitrotoluene equivalents.
2. D. T. Griggs, F. J. Turner, H. C. Heard, *Geol. Soc. Am. Mem.* **79**, 65 (1960).
3. M. S. Paterson and L. E. Weiss, *Nature* **198**, 1046 (1962).
4. J. G. Ramsey, *Geol. Mag.* **99**, 516 (1962).
5. H. E. McKinstry, *Am. J. Sci.* **251**, 401 (1953).
6. J. D. Moody and M. J. Hill, *Bull. Geol. Soc. Am.* **67**, 1207 (1956).
7. "Mathematically, a shock wave is an actual discontinuity propagating with a velocity greater than the local sound velocity," E. H. Freedman and E. F. Green, in *American Institute of Physics Handbook*, D. E. Gray, Ed. (McGraw-Hill, New York, 1957), pp. 2–231.
8. S. Glasstone, Ed., *The Effects of Nuclear Weapons* (U.S. Atomic Energy Commission, Washington, D.C., 1962), p. 104.
9. Work done on behalf of the U.S. Atomic Energy Commission. Publication authorized by the Director, U.S. Geological Survey. I thank the Lawrence Radiation Laboratory for providing the core samples.
* Present address: Astrogeological Branch, U.S. Geological Survey, Flagstaff, Arizona.

8 February 1964

Growth Layers on Ammonium Dihydrogen Phosphate

Abstract. *Microscopic observations of growth layers and etch pits on ammonium dihydrogen phosphate crystals reveal screw dislocations on the {100} face generating elliptical spirals that change rapidly but reversibly to rectangular shape when chromium-ion impurity is added. The effects of the impurity on crystal habit are judged to be secondary to changes in the morphology of the growth layers. No sources of growth are observed on the {101} faces; the layers spread inward from the edges and at times are mutually annihilating so that, temporarily, no steps are observed. Similar behavior is recorded for the {10$\bar{1}$1} faces of $NaNO_3$.*

Bunn and Emmett (*1*) stimulated interest in the formation of growth layers at the same time that Frank (*2*) suggested that crystal dislocations could provide the sources of steps required for continuous crystal growth. Albon and Dunning (*3*) developed a particularly fine experimental technique for the observation of layer morphology and growth kinetics of sucrose. Their methods have been emulated and extended in our investigation of the mechanism of growth of ammonium d[...] drogen phosphate crystals from aq[...] solution. In particular, we studied [...] nature of the deposition process [...] self, whether by surface nucleation [...] as initiated at dislocation sites, [...] as influenced by impurities.

In experiments with crystals that [...] nucleated more readily than suc[...] the chief difficulty arises from the [...] currence of spontaneous growth [...] tubes connecting the storage vessel [...] the growth cell. Undue heating [...] these leads necessarily interferes [...] precise temperature control in the [...]

The crystals were grown in a [...] (3-mm) cell consisting of top and b[...] tom (black) glass plates of op[...] quality, secured in a gold-plated b[...] block. Inlet and outlet tubes all[...] the circulation of salt solution from [...] external, carefully lagged, st[...] thermostat (40°C) by means of a [...] able peristaltic pump. Housed in a p[...] (methyl methacrylate) container, [...] cell could be rotated about the axis [...] the microscope tube and given [...] degree of tilt so that a particular [...] of a crystal could be brought into p[...] tion to be strongly illuminated b[...] focused beam of light. Photom[...] graphs were taken with a 35-mm si[...] lens reflex camera and with fine-g[...] film. For cine-film recording we us[...] 16-mm camera and reversal film.

Heat was supplied to or withdr[...] from the growth cell by means [...] Peltier junction attached to the b[...] of the cell. Thus the temperature [...] the cell could be raised or lowered [...] increase super- or undersaturation [...] desired. While unintentional temp[...] ture fluctuations in the cell [...] amounted to a few thousandths [...] degree Celsius, as measured [...] a platinum resistance thermom[...] it was suspected that fluctuations [...] the solutions tended to be some[...] greater.

We found that growth on the [...] face of ammonium dihydrogen p[...] phate crystals proceeds by a s[...] dislocation mechanism. The s[...] are roughly elliptical in shape [...] centricity about 0.86) and or[...] with the short axis of the ellipse p[...] lel to the [001] axis of the cr[...] Growth proceeds by the movem[...] steps across the crystal face. Th[...] are of varying height, visibility [...] roughly proportional to the step h[...] Occasionally we found single spir[...] in Fig. 1. However, most freq[...]